

Mathematical Modeling of the Kinetics of the Extrinsic Blood Coagulation System with Stoichiometric Anticoagulants

Zoltan Mester

Department of Chemical Engineering, University of Massachusetts Amherst

Joseph Powers and Samuel Paolucci

Department of Aerospace and Mechanical Engineering, University of Notre Dame

Summer 2007



Abstract



A mathematical model for the production of protein species within the extrinsic blood coagulation cascade originally developed by Hockin et al. is re-derived. The model consists of 34 differential equations that describe the rate of production of each protein species, and is obtained by treating each of the 27 independent chemical equilibrium expressions ~~in the cascade~~ as elementary reactions. This model allows for the exploration of the dynamics of blood coagulation in a time efficient manner and for the observation of protein concentrations that are below detection limits by physical analysis. From this model, the concentrations of protein species as a function of time are obtained. The effects of changing the initial concentrations of certain protein species on blood coagulation are simulated and the results are discussed in light of empirical knowledge about the coagulation cascade. An attempt is made to simplify the computations needed to solve the system by finding the attracting invariant low-dimensional manifold of the system, which is a low-dimensional path that all trajectories leading to the same equilibrium point follow once the fast time-scales in the system have equilibrated. It is found that increasing factor VII concentration in the blood stream has an inhibiting effect on the production of thrombin (factor IIa), and hence inhibits coagulation. Coagulation is promoted by the addition of factor VIIa in the blood. The essential role of antithrombin III (ATIII) and TFPI in the termination of coagulation is also demonstrated. Cases of hemophilia A and B are also simulated with our model. The invariant one-dimensional manifold is found to be of use in simplifying the system between reaction times of 4000 and 40000 seconds.

1 Introduction

This paper discusses the biochemistry of blood coagulation and presents the chemical reactions involved in the coagulation cascade that was originally developed by Hockin et al [1]. The mathematics of systems of ordinary differential equations and invariant low-dimensional manifolds are discussed. The mathematical work done to perform the analysis on the blood coagulation model is presented and the ordinary differential equations that model coagulation and that were originally derived by Hockin et al. are re-derived. Relevant concentration versus time graphs are included and the effects of changing certain parameters on blood coagulation are discussed. The system dynamics is explored by including projections of the invariant low dimensional manifold and graphing the time-scales of the system for all reaction times.

Blood coagulation takes place via a cascade of chemical reactions involving pro- and anticoagulant systems in order to maintain proper blood fluidity [1]. Deficiencies or excesses in the proteins involved in coagulation can lead to hemorrhagic or thrombotic diseases [1]. Looking at the chemical properties of isolated proteins ignores the dynamic interplay between several species and often results in faulty predictions about the effects of changing protein concentrations [1]. For example, if the concentration of VII, a procoagulant factor, is increased, one would expect clotting time to decrease, yet experiments show the opposite to be true [1, 2]. Mathematical models are a powerful tool to explore the dynamics of the interplay between several protein species involved in coagulation. Mathematical models provide a quicker way to demonstrate this interplay than experiment and can examine species concentrations below detection limits [1].

Previous work on the mathematical modeling of blood coagulation looked at the time-dependent concentrations of each species obtained from a limited set of initial conditions [1, 3]. This work involved treating each reaction in the coagulation cascade as an elementary chemical reaction and using the law of mass action to derive nonlinear differential equations that describe the rate of production of each protein species [1, 3]. We repeat this work by re-deriving this set of differential equations. This set of differential equations is simplified to get a set of differential algebraic equations and numerical solutions for the time-dependent concentrations are obtained. The initial conditions for several protein species are varied in an attempt to simulate various clotting disorders and the results are compared to empirical knowledge. Hemophilia A and B and antithrombin III (ATIII) and tissue factor pathway inhibitor (TFPI) deficiency are simulated and the possible treatment of hemorrhagic diseases with factor VII and VIIa are explored. A study of the dynamics of the system is performed by obtaining the equilibrium points, linearizing the system of differential equations near the physical equilibrium point, and solving for the time-scales that govern the system dynamics at physical equilibrium. The time-scales over the whole reaction time are obtained and their effects on the system dynamics is discussed. An attempt is made to simplify the system by finding the attracting invariant low-dimensional manifold.

2 Blood Coagulation

Blood coagulation takes place via extrinsic and intrinsic pathways [4]. Both pathways lead to the production of thrombin (factor IIa), which is involved in the conversion of soluble fibrinogen found in blood into a fibrin meshwork [4]. This fibrin meshwork, in conjunction with platelets, plugs the site of the injury until tissue repair is complete. The biological significance of the intrinsic pathway remains suspect because individuals missing key proteins in the sequence show no bleeding disorders [5]. Therefore, our work focuses on the

Table 1: Chemical expressions for the coagulation cascade

Line	Chemical expressions
1	$\text{TF} + \text{VII} < 1 - 2 > \text{TF} = \text{VII}$
2	$\text{TF} + \text{VIIa} < 3 - 4 > \text{TF} = \text{VIIa}$
3	$\text{TF} = \text{VIIa} + \text{VII} - 5 > \text{TF} = \text{VIIa} + \text{VIIa}$
4	$\text{Xa} + \text{VII} - 6 > \text{Xa} + \text{VIIa}$
5	$\text{IIa} + \text{VII} - 7 > \text{IIa} + \text{VIIa}$
6	$\text{TF} = \text{VIIa} + \text{X} < 8 - 9 > \text{TF} = \text{VIIa} = \text{X} - 10 > \text{TF} = \text{VIIa} = \text{Xa}$
7	$\text{TF} = \text{VIIa} + \text{Xa} < 11 - 12 > \text{TF} = \text{VIIa} = \text{Xa}$
8	$\text{TF} = \text{VIIa} + \text{IX} < 13 - 14 > \text{TF} = \text{VIIa} = \text{IX} - 15 > \text{TF} = \text{VIIa} + \text{IXa}$
9	$\text{Xa} + \text{II} - 16 > \text{Xa} + \text{IIa}$
10	$\text{IIa} + \text{VIII} - 17 > \text{IIa} + \text{VIIIa}$
11	$\text{VIIIa} + \text{IXa} < 18 - 19 > \text{IXa} = \text{VIIIa}$
12	$\text{IXa} = \text{VIIIa} + \text{X} < 20 - 21 > \text{IXa} = \text{VIIIa} = \text{X} - 22 > \text{IXa} = \text{VIIIa} + \text{Xa}$
13	$\text{VIIIa} < 23 - 24 > \text{VIIIa}_1 \cdot \text{L} + \text{VIIIa}_2$
14	$\text{IXa} = \text{VIIIa} = \text{X} - 25 > \text{VIIIa}_1 \cdot \text{L} + \text{VIIIa}_2 + \text{X} + \text{IXa}$
15	$\text{IXa} = \text{VIIIa} - 25 > \text{VIIIa}_1 \cdot \text{L} + \text{VIIIa}_2 + \text{IXa}$
16	$\text{IIa} + \text{V} - 26 > \text{IIa} + \text{Va}$
17	$\text{Xa} + \text{Va} < 27 - 28 > \text{Xa} = \text{Va}$
18	$\text{Xa} = \text{Va} + \text{II} < 29 - 30 > \text{Xa} = \text{Va} = \text{II} - 31 > \text{Xa} = \text{Va} + \text{mIIa}$
19	$\text{mIIa} + \text{Xa} = \text{Va} - 32 > \text{IIa} + \text{Xa} = \text{Va}$
20	$\text{Xa} + \text{TFPI} < 33 - 34 > \text{Xa} = \text{TFPI}$
21	$\text{TF} = \text{VIIa} = \text{Xa} + \text{TFPI} < 35 - 36 > \text{TF} = \text{VIIa} = \text{Xa} = \text{TFPI}$
22	$\text{TF} = \text{VIIa} + \text{Xa} = \text{TFPI} - 37 > \text{TF} = \text{VIIa} = \text{Xa} = \text{TFPI}$
23	$\text{Xa} + \text{ATIII} - 38 > \text{Xa} = \text{ATIII}$
24	$\text{mIIa} + \text{ATIII} - 39 > \text{mIIa} = \text{ATIII}$
25	$\text{IXa} + \text{ATIII} - 40 > \text{IXa} = \text{ATIII}$
26	$\text{IIa} + \text{ATIII} - 41 > \text{IIa} = \text{ATIII}$
27	$\text{TF} = \text{VIIa} + \text{ATIII} - 42 > \text{TF} = \text{VIIa} + \text{ATIII}$

extrinsic pathway. The reaction mechanism for the extrinsic pathway of blood coagulation can be found in Table 1 [1].¹

Blood coagulation starts by the contact of tissue factor (TF), a transmembrane protein, with enzymes circulating in the blood stream [2,4]. When a blood vessel is damaged, TF, found in the membranes of cells not normally in contact with blood, comes into contact with the activated coagulant factor VIIa, forming the VIIa-TF complex (Table 1, line 2) [2,5]. VIIa-TF in turn activates factors X and IX to form Xa and IXa by limited proteolysis (Table 1, lines 6, 7, and 8) [2]. Factor IXa combines with factor VIIIa to form a

¹The notation $-2 >$ signifies the forward reaction with specific reaction rate k_2 . The notation $< 1 - 2 >$ indicates an equilibrium expression with specific reaction rate k_1 for the reverse and specific reaction rate k_2 for the forward reaction. The notation $=$ indicates binding between two components.

secondary pathway to activate factor X (Table 1, lines 11 and 12) [2]. Factor Xa formed by these processes activates factor II to form thrombin (factor IIa) (Table 1, line 9) [1]. Thrombin is further produced via the thrombin-led activation of factor V to form Va (Table 1, line 16) [1]. Va binds with Xa to form the Va-Xa complex, which activates II to form meizothrombin (mIIa) (Table 1, lines 17, and 18) [1]. mIIa is converted into IIa by the Va-Xa complex (Table 1, line 19) [1]. In the mean time, more VIIa is formed by the activation of VII in a self-propagating loop (Table 1, line 3) [1]. VII is further activated by thrombin and factor Xa (Table 1, lines 4 and 5) [1].

Antithrombin III and TFPI are the main inhibitors of thrombin and other enzymes involved in thrombin production [1]. Because the inability of the body to control the amount of active thrombin in the blood stream could lead to thrombosis, the presence of these inhibitors is crucial. ATIII functions by forming complexes with Xa, mIIa, IXa, IIa, and TF=VIIa (Table 1, lines 23-27) [1]. TFPI functions by inhibiting the Xa-VIIa-TF complex (Table 1, line 21) and by binding to Xa to form the TFPI-Xa complex, which in turn binds to TF=VIIa (Table 1, lines 20 and 22).

3 Mathematics

3.1 Systems of Ordinary Differential Equations

A system of n first order ordinary differential equations can be written as

$$\frac{d\mathbf{x}}{dt} = \mathbf{f}(x_1, x_2, \dots, x_n), \quad (1)$$

where \mathbf{f} vector contains the functions that describe the rates of change of the dependent variables, t is the independent variable, \mathbf{x} is a vector of dependent variables of length n , and x_i are the individual dependent variables. A linear system of differential equations can be written as

$$\frac{d\mathbf{x}}{dt} = \mathbf{A} \cdot \mathbf{x}, \quad (2)$$

where \mathbf{A} is a constant matrix. The solution to equation (2) takes the form

$$\mathbf{x}(t) = \sum_{i=1}^n \mathbf{g}_i e^{\lambda_i t}, \quad (3)$$

where λ_i are the eigenvalues of \mathbf{A} with \mathbf{g}_i being the corresponding eigenvectors.

A technique used to analyze a problem involving a system of nonlinear first order ordinary differential equations is to linearize the system about some point \mathbf{x}_0 [6]. This is done by calculating the Jacobian of the system about \mathbf{x}_0 [6]. The Jacobian about \mathbf{x}_0 is

$$\mathbf{J} = \begin{pmatrix} \frac{\partial f_1}{\partial x_1} & \frac{\partial f_1}{\partial x_2} & \cdots & \frac{\partial f_1}{\partial x_n} \\ \frac{\partial f_2}{\partial x_1} & \frac{\partial f_2}{\partial x_2} & \cdots & \frac{\partial f_2}{\partial x_n} \\ \vdots & \vdots & \ddots & \vdots \\ \frac{\partial f_n}{\partial x_1} & \frac{\partial f_n}{\partial x_2} & \cdots & \frac{\partial f_n}{\partial x_n} \end{pmatrix}, \quad (4)$$

where f_i are elements of vector \mathbf{f} . The linearized system takes the form

$$\frac{d\mathbf{x}}{dt} = \mathbf{J} \cdot \mathbf{x}, \quad (5)$$

where \mathbf{J} takes the place of \mathbf{A} in equation (2). The solution of equation (5) is in the form of equation (3) and λ_i are the eigenvalues of the Jacobian about \mathbf{x}_0 and \mathbf{g}_i are the corresponding eigenvectors. The time-scales of the system are given by [7]

$$\tau_i = \frac{1}{|Re(\lambda_i)|}, \quad (6)$$

where $Re(\lambda_i)$ is the real part of the eigenvalue λ_i . The fast time-scales only influence the behavior of the system at the initial times and at longer times the slow time-scales alone govern the behavior of the system. The long time-scale can be observed in the system response.

The equilibrium points, where the rates of change of the dependent variables are equal to zero, can also be found for a set of independent first order ordinary differential equations. This is done by solving the following equation:

$$\mathbf{f}(x_1, x_2, \dots, x_n) = \mathbf{0}. \quad (7)$$

A non-linear system may have multiple equilibria and some might be unstable nodes or saddle points. If the Jacobian around the equilibrium point yields all negative and zero eigenvalues, we have a stable node. If all the eigenvalues are positive with possibly some zeros, we have an unstable node. A saddle point is present if some of the eigenvalues are positive and some are negative.

3.2 Invariant Low-Dimensional Manifolds

To analyze the dynamics of complex reaction systems, it can be useful to look at the trajectories of the reaction system through phase space. For a high dimensional system with an attracting low-dimensional manifold, which is a lower dimensional surface ($< R^n$) that attracts all trajectories, the trajectories approach one another before the equilibrium is reached [8]. A one-dimensional manifold is a curve.

Attracting low-dimensional manifolds arise from the different time-scales present in the system. A set of n independent first order linear ordinary differential equations, as in equation (2), has n different time scales associated with it. Initially, when all time-scales play a role in the dynamics of the system, the trajectories take a path through an n -dimensional space. As time increases, the effects of the fast time-scales on the system decrease and the trajectories of the system take a path through lower-dimensional space. When the slowest time-scale dominates the system, the trajectories follow a one-dimensional manifold, or a curve.

Whether a path through the phase space qualifies as an attracting manifold depends upon the eigenvalues computed from the Jacobian along that path. Perturbing the system away from the manifold can yield the following results [8]:

1. Perturbing in the direction of an eigenvector with a corresponding positive eigenvalue makes the perturbation grow and the trajectory move away from the given path.
2. Perturbing in the direction of an eigenvector with a corresponding 0 eigenvalue causes no change in the perturbation.
3. Perturbing in the direction of an eigenvector with a corresponding negative eigenvalue makes the perturbation go to 0 and the trajectory moves back to the given path.

An attracting manifold is one that has all negative eigenvalues, with possibly some 0 eigenvalues, associated with it. This guarantees that all trajectories are drawn to it as time increases. Attracting low-dimensional

manifolds in effect provide a simplification for a complex system because once the fast time-scales have equilibrated the trajectories of the system are consigned to a low-dimensional path with fewer degrees of freedom.

3.3 Law of Mass Action

An elementary chemical reaction, a reaction that occurs in a single step with no reaction intermediates, where species X combines with species Y to form species P is written as



where a , b , and c are stoichiometric coefficients.

For a species that is consumed, such as species X , the rate at which the species is consumed, $d[X]/dt$, can be modeled via the law of mass action as

$$\frac{d[X]}{dt} = -k[X]^a[Y]^b, \quad (9)$$

where the brackets indicate the concentration of the species within the brackets and k is the specific reaction rate. The negative sign preceding the rate constant indicates that the species is consumed.

For a species that is produced, such as species P , the rate at which the species is consumed, $d[P]/dt$, can be modeled via the law of mass action as

$$\frac{d[P]}{dt} = k[X]^a[Y]^b. \quad (10)$$

For species involved in multiple reactions, the right hand sides of the rate equations for each reaction are added. For example, for X in



the rate equation is written as

$$\frac{d[X]}{dt} = -k_1[X]^a[Y]^b + k_2[Z], \quad (13)$$

where k_1 refers to the rate constant for the first reaction, equation (11), and k_2 refers to the rate constant for the second reaction, equation (12). The law of mass action can be applied to both the forward and reverse reaction of an equilibrium reaction.

3.4 Application to Blood Coagulation

Each reaction in the blood coagulation cascade is assumed to be an elementary chemical reaction and the differential equations for the rate of production of each species as proposed by Hockin et al. is re-derived using the law of mass action. The following equations represent the rate of production of each species:

$$\begin{aligned} \frac{d[TF]}{dt} = & k_1[TF = VII] - k_2[TF][VII] + k_3[TF = VIIa] \\ & - k_4[TF][VIIa], \end{aligned} \quad (14)$$

$$\begin{aligned} \frac{d[VII]}{dt} &= k_1[TF = VII] - k_2[TF][VII] - k_5[TF = VIIa][VII] \\ &\quad - k_6[Xa][VII] - k_7[IIa][VII], \end{aligned} \quad (15)$$

$$\frac{d[TF = VII]}{dt} = -k_1[TF = VII] + k_2[TF][VII], \quad (16)$$

$$\begin{aligned} \frac{d[VIIa]}{dt} &= k_3[TF = VIIa] - k_4[TF][VIIa] + k_5[TF = VIIa][VII] \\ &\quad + k_6[Xa][VII] + k_7[IIa][VII] \end{aligned} \quad (17)$$

$$\begin{aligned} \frac{d[TF = VIIa]}{dt} &= -k_3[TF = VIIa] + k_4[TF][VIIa] + k_8[TF = VIIa = X] \\ &\quad - k_9[TF = VIIa][X] + k_{11}[TF = VIIa = Xa] \\ &\quad - k_{12}[TF = VIIa][Xa] + k_{13}[TF = VIIa = IX] \\ &\quad - k_{14}[TF = VIIa][IX] + k_{15}[TF = VIIa = IX] \\ &\quad - k_{37}[TF = VIIa][Xa = TFPI] \\ &\quad - k_{42}[TF = VIIa][ATIII], \end{aligned} \quad (18)$$

$$\begin{aligned} \frac{d[Xa]}{dt} &= k_{11}[TF = VIIa = Xa] - k_{12}[TF = VIIa][Xa] \\ &\quad + k_{22}[IXa = VIIa = X] + k_{27}[Xa = Va] - k_{28}[Xa][Va] \\ &\quad + k_{33}[Xa = TFPI] - k_{34}[Xa][TFPI] - k_{38}[Xa][ATIII], \end{aligned} \quad (19)$$

$$\frac{d[IIa]}{dt} = k_{16}[Xa][II] + k_{32}[mIIa][Xa = Va] - k_{41}[IIa][ATIII], \quad (20)$$

$$\begin{aligned} \frac{d[X]}{dt} &= k_8[TF = VIIa = X] - k_9[TF = VIIa][X] \\ &\quad + k_{20}[IXa = VIIa = X] - k_{21}[IXa = VIIa][X] \\ &\quad + k_{25}[IXa = VIIa = X], \end{aligned} \quad (21)$$

$$\begin{aligned} \frac{d[TF = VIIa = X]}{dt} &= -k_8[TF = VIIa = X] + k_9[TF = VIIa][X] \\ &\quad - k_{10}[TF = VIIa = X], \end{aligned} \quad (22)$$

$$\begin{aligned} \frac{d[TF = VIIa = Xa]}{dt} &= k_{10}[TF = VIIa = X] - k_{11}[TF = VIIa = Xa] \\ &\quad + k_{12}[TF = VIIa][Xa] + k_{35}[TF = VIIa = Xa = TFPI] \\ &\quad - k_{36}[TF = VIIa = Xa][TFPI], \end{aligned} \quad (23)$$

$$\frac{d[IX]}{dt} = k_{13}[TF = VIIa = IX] - k_{14}[IX][TF = VIIa], \quad (24)$$

$$\begin{aligned} \frac{d[TF = VIIa = IX]}{dt} &= -k_{13}[TF = VIIa = IX] + k_{14}[IX][TF = VIIa] \\ &\quad - k_{15}[TF = VIIa = IX], \end{aligned} \quad (25)$$

$$\frac{d[VIII]}{dt} = -k_{17}[IIa][VIII], \quad (26)$$

$$\begin{aligned} \frac{d[VIIIa]}{dt} &= k_{17}[IIa][VIII] + k_{18}[IXa = VIIIa] \\ &\quad - k_{19}[VIIIa][IXa] + k_{23}[VIIIa_1 \cdot L][VIIIa_2] \\ &\quad - k_{24}[VIIIa], \end{aligned} \quad (27)$$

$$\begin{aligned} \frac{d[IXa]}{dt} &= k_{15}[TF = VIIa = IX] + k_{18}[IXa = VIIIa] \\ &\quad - k_{19}[VIIIa][IXa] + k_{25}[IXa = VIIIa = X] \end{aligned}$$

$$+k_{25}[IXa = VIIIa] - k_{40}[IXa][ATIII], \quad (28)$$

$$\begin{aligned} \frac{d[IXa = VIIIa]}{dt} &= -k_{18}[IXa = VIIIa] + k_{19}[IXa][VIIIa] \\ &+ k_{20}[IXa = VIIIa = X] - k_{21}[IXa = VIIIa][X] \\ &+ k_{22}[IXa = VIIIa = X] - k_{25}[IXa = VIIIa], \end{aligned} \quad (29)$$

$$\begin{aligned} \frac{d[IXa = VIIIa = X]}{dt} &= -k_{20}[IXa = VIIIa = X] + k_{21}[IXa = VIIIa][X] \\ &- k_{22}[IXa = VIIIa = X] - k_{25}[IXa = VIIIa = X], \end{aligned} \quad (30)$$

$$\begin{aligned} \frac{d[VIIIa_1 \cdot L]}{dt} &= -k_{23}[VIIIa_1 \cdot L][VIIIa_2] \\ &+ k_{24}[VIIIa] + k_{25}[IXa = VIIIa = X] \\ &+ k_{25}[IXa = VIIIa], \end{aligned} \quad (31)$$

$$\begin{aligned} \frac{d[VIIIa_2]}{dt} &= -k_{23}[VIIIa_1 \cdot L][VIIIa_2] + k_{24}[VIIIa] \\ &+ k_{25}[IXa = VIIIa = X] + k_{25}[IXa = VIIIa], \end{aligned} \quad (32)$$

$$\frac{d[V]}{dt} = -k_{26}[IIa][Va], \quad (33)$$

$$\begin{aligned} \frac{d[Va]}{dt} &= k_{26}[IIa][Va] + k_{27}[Xa = Va] \\ &- k_{28}[Xa][Va], \end{aligned} \quad (34)$$

$$\begin{aligned} \frac{d[Xa = Va]}{dt} &= -k_{27}[Xa = Va] + k_{28}[Xa][Va] \\ &+ k_{29}[Xa = Va = II] - k_{30}[Xa = Va][II] \\ &+ k_{31}[Xa = Va = II], \end{aligned} \quad (35)$$

$$\begin{aligned} \frac{d[II]}{dt} &= -k_{16}[Xa][II] + k_{29}[Xa = Va = II] \\ &- k_{30}[Xa = Va][II], \end{aligned} \quad (36)$$

$$\begin{aligned} \frac{d[Xa = Va = II]}{dt} &= -k_{29}[Xa = Va = II] + k_{30}[Xa = Va][II] \\ &- k_{31}[Xa = Va = II], \end{aligned} \quad (37)$$

$$\begin{aligned} \frac{d[mIIa]}{dt} &= k_{31}[Xa = Va = II] - k_{32}[mIIa][Xa = Va] \\ &- k_{39}[mIIa][ATIII], \end{aligned} \quad (38)$$

$$\begin{aligned} \frac{d[TFPI]}{dt} &= k_{33}[Xa = TFPI] - k_{34}[Xa][TFPI] \\ &+ k_{35}[TF = VIIa = Xa = TFPI] \\ &- k_{36}[TF = VIIa = Xa][TFPI], \end{aligned} \quad (39)$$

$$\begin{aligned} \frac{d[Xa = TFPI]}{dt} &= -k_{33}[Xa = TFPI] + k_{34}[Xa][TFPI] \\ &- k_{37}[TF = VIIa][Xa = TFPI], \end{aligned} \quad (40)$$

$$\begin{aligned} \frac{d[TF = VIIa = Xa = TFPI]}{dt} &= -k_{35}[TF = VIIa = Xa = TFPI] \\ &+ k_{36}[TF = VIIa = Xa][TFPI] \\ &+ k_{37}[TF = VIIa][Xa = TFPI], \end{aligned} \quad (41)$$

$$\begin{aligned} \frac{d[ATIII]}{dt} &= -k_{38}[Xa][ATIII] - k_{39}[mIIa][ATIII] - k_{40}[IXa][ATIII] \\ &- k_{41}[IIa][ATIII] - k_{42}[TF = VIIa][ATIII], \end{aligned} \quad (42)$$

$$\frac{d[Xa = ATIII]}{dt} = k_{38}[Xa][ATIII], \quad (43)$$

$$\frac{d[mIIa = ATIII]}{dt} = k_{39}[mIIa][ATIII], \quad (44)$$

$$\frac{d[IXa = ATIII]}{dt} = k_{40}[IXa][ATIII], \quad (45)$$

$$\frac{d[IIa = ATIII]}{dt} = k_{41}[IIa][ATIII], \quad (46)$$

$$\frac{d[TF = VIIa = ATIII]}{dt} = k_{42}[TF = VIIa][ATIII], \quad (47)$$

where the variables within the brackets indicate concentrations of protein species. The rate constants have values found in the literature [1]. The above system, equations (14-47), can be written in the following form:

$$\frac{d\mathbf{y}}{dt} = \mathbf{C} \cdot \mathbf{g}(\mathbf{y}), \quad (48)$$

where \mathbf{C} is a constant matrix, \mathbf{y} is a vector with

$$\mathbf{y} = \begin{pmatrix} [\text{TF}] \\ [\text{VII}] \\ \vdots \\ [\text{TF=VIIa=ATIII}] \end{pmatrix}, \quad (49)$$

and $\mathbf{g}(\mathbf{y})$ is a vector with

$$\mathbf{g}(\mathbf{y}) = \begin{pmatrix} k_1[TF = VII] \\ k_2[TF][VII] \\ \vdots \\ k_{42}[TF = VIIa][ATIII] \end{pmatrix}. \quad (50)$$

The system of differential equations represented by equation (48) is not an independent system. The system can be reduced by finding algebraic constraints that eliminate some of the differential equations. The system represented by equation (48) is reduced by rearranging matrix \mathbf{C} into row-echelon form through a matrix decomposition. \mathbf{C} is decomposed to get

$$\mathbf{C} = \mathbf{L} \cdot \mathbf{P} \cdot \mathbf{Q} \cdot \mathbf{U}, \quad (51)$$

where \mathbf{L} is a lower triangular matrix. A MATLAB program, written by the author, is used to perform the decomposition. First \mathbf{C} is decomposed via an LU decomposition into a lower and upper triangular matrix, then the upper triangular matrix is decomposed into a pseudo-row-echelon matrix, \mathbf{U} , and two other matrices, \mathbf{P} and \mathbf{Q} . \mathbf{U} is referred to as a pseudo-row-echelon matrix because it has all the characteristics of a row-echelon matrix except the rows are not in the standard order. Equation (51) is substituted into equation (48) and $\mathbf{U} \cdot \mathbf{g}(\mathbf{y})$ is solved for in the following way:

$$\mathbf{U} \cdot \mathbf{g}(\mathbf{y}) = \mathbf{Q}^{-1} \cdot \mathbf{P}^{-1} \cdot \mathbf{L}^{-1} \cdot \frac{d\mathbf{y}}{dt}. \quad (52)$$

The equations with 0 for the left hand side are selected from equation (52). These are the algebraic constraints of our system. An example of such an algebraic constraint is

$$0 = -\frac{d[TF]}{dt} + \frac{d[VII]}{dt} + \frac{d[VIIa]}{dt}. \quad (53)$$

Equation (53) is integrated from the initial concentrations to the final concentrations of each species to get

$$0 = -[TF] + [TF]_0 + [VII] - [VII]_0 + [VIIa] - [VIIa]_0, \quad (54)$$

where the variables with the subscript 0 are the initial concentrations of the proteins. The other 9 algebraic constraints are similarly derived and the system of 10 algebraic equations are simplified with the MATHEMATICA software. These are the 10 simplified algebraic equations:

$$[VIIa] = -[TF]_0 + [VII]_0 + [VIIa]_0 + [TF] - [VII], \quad (55)$$

$$\begin{aligned} [VIIIa_1 \cdot L] &= [VIII]_0 + [VIIIa]_0 + [IXa = VIIIa]_0 \\ &+ [IXa = VIIIa = X]_0 + [VIIIa_1 \cdot L]_0 - [VIII] - [VIIIa] \\ &- [IXa = VIIIa] - [IXa = VIIIa = X], \end{aligned} \quad (56)$$

$$\begin{aligned} [VIIIa_2] &= [VIII]_0 + [VIIIa]_0 + [IXa = VIIIa]_0 + [IXa = VIIIa = X]_0 \\ &+ [VIIIa_2]_0 - [VIII] - [VIIIa] - [IXa = VIIIa] \\ &- [IXa = VIIIa = X], \end{aligned} \quad (57)$$

$$\begin{aligned} [Xa = Va = II] &= [V]_0 + [Va]_0 + [Xa = Va]_0 + [Xa = Va = II]_0 - [V] - [Va] \\ &- [Xa = Va], \end{aligned} \quad (58)$$

$$\begin{aligned} [TF = VIIa = Xa = TFPI] &= [TFPI]_0 + [Xa = TFPI]_0 + [TF = VIIa = Xa = TFPI]_0 \\ &- [TFPI] - [Xa = TFPI], \end{aligned} \quad (59)$$

$$\begin{aligned} [ATIII] &= -2[TF = VIIa = Va]_0 - [IX]_0 - 2[TF = VIIa = IX]_0 \\ &- [IXa = VIIIa]_0 - 2[IXa = VIIIa = X]_0 - [TF]_0 - [IXa]_0 \\ &+ 2[V]_0 + 2[Va]_0 + [Xa = Va]_0 - [II]_0 - [mIIa]_0 + 2[TFPI]_0 \\ &+ [ATIII]_0 - [TF = VII]_0 - [TF = VIIa]_0 - [Xa]_0 \\ &- [IIa]_0 - [X]_0 - 2[TF = VIIa = X]_0 + [Xa = TFPI]_0 + [TF] \\ &+ 2[TF = VIIa = Xa] + [IX] + 2[TF = VIIa = IX] + [IXa] \\ &- [Xa = Va] + [II] + [mIIa] - 2[TFPI] - [Xa = TFPI] \\ &+ [IXa = VIIIa] + 2[IXa = VIIIa = X] + [TF = VII] \\ &+ [TF = VIIa] + [Xa] + [IIa] + [X] \\ &+ 2[TF = VIIa = X] - 2[V] - 2[Va], \end{aligned} \quad (60)$$

$$\begin{aligned} [Xa = ATIII] &= [TF = VIIa = Xa]_0 + [IXa = VIIIa = X]_0 - [V]_0 - [Va]_0 \\ &- [TFPI]_0 + [Xa = ATIII]_0 + [Xa]_0 + [X]_0 + [TF = VIIa = X]_0 \\ &- [TF = VIIa = Xa] - [IXa = VIIIa = X] + [V] + [Va] \\ &+ [TFPI] - [Xa] - [X] - [TF = VIIa = X], \end{aligned} \quad (61)$$

$$\begin{aligned} [IXa = ATIII] &= [IX]_0 + [TF = VIIa = IX]_0 + [IXa]_0 \\ &+ [IXa = VIIIa]_0 + [IXa = VIIIa = X]_0 + [IXa = ATIII]_0 \\ &- [IX] - [TF = VIIa = IX] - [IXa] - [IXa = VIIIa] \\ &- [IXa = VIIIa = X], \end{aligned} \quad (62)$$

$$[IIa = ATIII] = -[V]_0 - [Va]_0 - [Xa = Va]_0 + [II]_0$$

$$\begin{aligned}
& +[mIIa]_0 + [mIIa = ATIII]_0 + [IIa = ATIII]_0 + [IIa]_0 + [V] \\
& +[Va] + [Xa = Va] - [II] - [mIIa] \\
& -[mIIa = ATIII] - [IIa], \tag{63}
\end{aligned}$$

$$\begin{aligned}
[TF = VIIa = ATIII] = & [TF = VIIa = Xa]_0 + [TF = VIIa = IX]_0 + [TF]_0 \\
& -[TFPI]_0 - 2[Xa = TFPI]_0 + [TF = VIIa = ATIII]_0 \\
& +[TF = VII]_0 + [TF = VIIa]_0 + [TF = VIIa = X]_0 \\
& -[TF = VIIa = IX] + [TFPI] + 2[Xa = TFPI] - [TF = VII] \\
& -[TF] - [TF = VIIa = Xa] \\
& -[TF = VIIa] - [TF = VIIa = X]. \tag{64}
\end{aligned}$$

Out of the differential equations obtained, 10 were replaced with the algebraic constraints that have matching species concentrations on the left hand side. These 34 differential algebraic equations are solved numerically using MATHEMATICA and concentration versus time graphs for each species are generated. A precision of 100 digits after the decimal point is required with the constants employed and a precision of 50 digits is required in the numerical solutions of the differential equations. These are chosen so that increasing the precision does not affect the solution.

The equilibrium points of the system are obtained by setting the right hand side of the 24 differential equations in the differential algebraic equation system equal to 0 and solving the system with the algebraic constraints. A numerical root finder in MATHEMATICA is used to obtain the roots of the system. Because we have a large, highly nonlinear system, we are unable to obtain all the roots using MATHEMATICA and we are unable to find any unstable nodes. The only root we are able to find is the stable one corresponding to the physical equilibrium since we use the species concentrations at large times as the initial guess for our root solver.

4 Results

4.1 In Vivo Coagulation under Normal Conditions

Log-log plots of concentration versus time of some key species are included in this report for conditions normally found in the body. Other plots are relegated to the Appendix. Unless otherwise noted, the initial conditions used are ones found in the literature [1].

The thrombin concentration versus time graph is examined because thrombin is necessary to convert fibrinogen into fibrin (Fig. 1a). The Xa concentration versus time graph is examined because Xa is responsible for activating prothrombin to become thrombin (Fig. 1b). It can be seen that from an initial concentration of 0, the amount of thrombin in the blood stream grows until it reaches its maximum around 300 seconds and then practically returns to 0 by 10,000 seconds as antithrombin III and TFPI inhibit its production and bind it. The Xa concentration increases as factor X is activated, but decreases and eventually reaches 0 as it is bound by antithrombin III.

The concentration versus time graphs are also examined for antithrombin III and TFPI (Fig. 2a and Fig. 2b). It can be observed that the antithrombin III concentration stays fairly constant near the initial value until there is a drop around 300 seconds. This coincides with the decrease in thrombin concentration

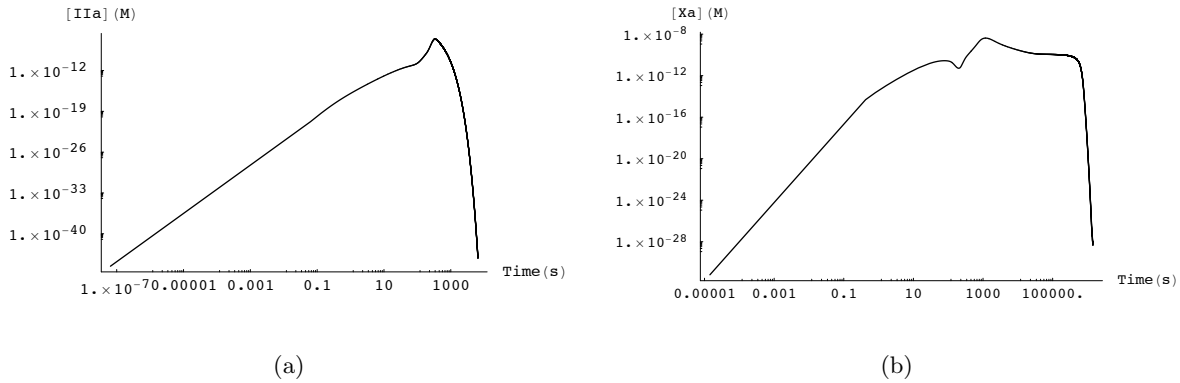


Fig. 1: Concentration as a function of time of (a) thrombin and (b) Xa.

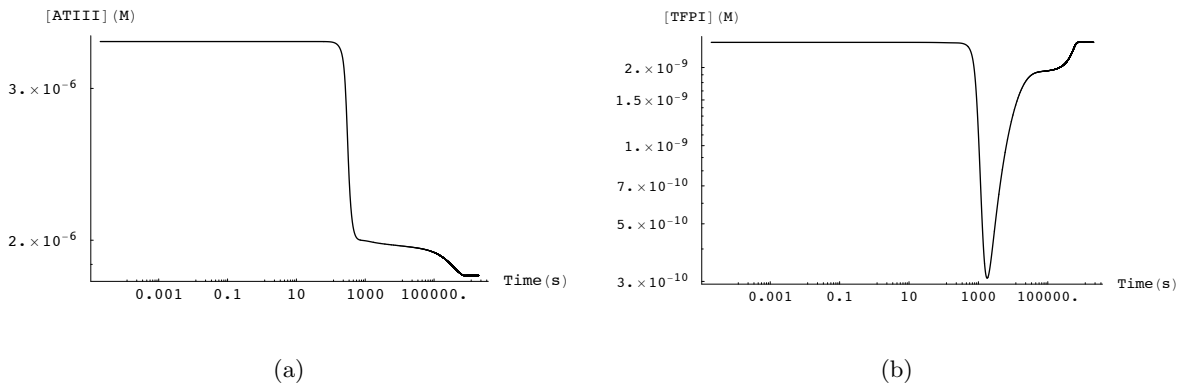


Fig. 2: Concentration as a function of time of (a) antithrombin III and (b) TFPI.

near 300 seconds, suggesting that thrombin production has started to be inhibited and thrombin has started to be bound by antithrombin III. TFPI shows the same dip in concentration around 300 seconds, but over large time-scales the concentration rises probably due to the reversible nature of the reactions involved.

Factor VIIa concentration versus time is examined since VIIa binding with TF is what starts the blood coagulation cascade (Fig. 3a). As VIIa complexes with TF to form VIIa-TF, VIIa concentration decreases initially. This decrease is by such a small amount that it cannot be demonstrated on the graph. However, the VIIa concentration later increases and reaches a nonzero equilibrium value probably due to the reversible nature of the chemical reactions.

The time-dependent concentration of complex VIIa-TF is graphed because this complex converts factor X into Xa (Fig. 3b). The concentration of complex VIIa-TF increases as it is generated by the binding of factors TF and VIIa. VIIa-TF is bound by ATIII leading to the decrease in VIIa-TF concentration at larger times that eventually leads to a concentration that is near 0. The dynamics of VIIa-TF consumption and production is complicated by several equilibrium expressions involving the binding of VIIa-TF with X, IX, and Xa. The decrease and increase in concentration at intermediate times may be a result of the complex interplay between the reactions that VIIa-TF is involved in.

The physically significant equilibrium values of all the species concentrations are obtained using the method described in Section 3. These values correspond to the values obtained for concentrations at large

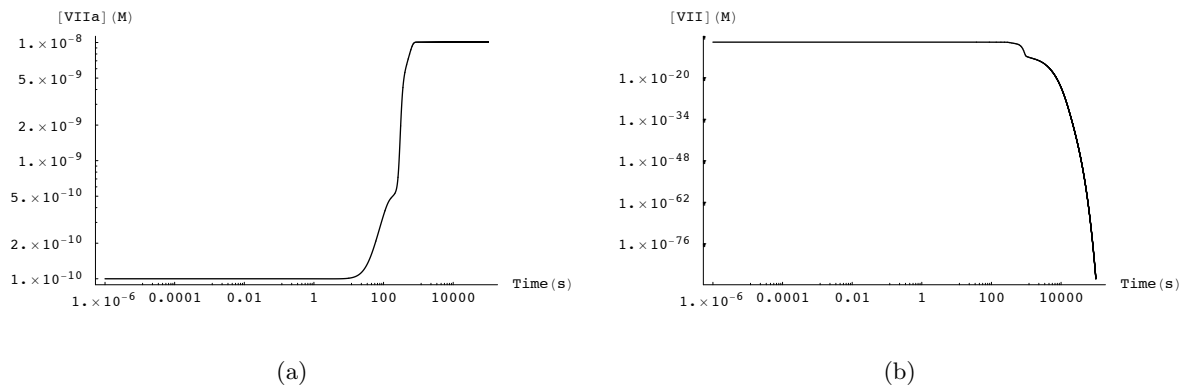


Fig. 3: Concentration as a function of time of (a) VIIa and (b) VIIa-TF.

times. The equilibrium concentrations can be found in Table 2.

Table 2: Equilibrium concentrations of all the protein species

Species	Concentration(M)	Species	Concentration(M)
[TF]	0	[VII]	0
[TF = VII]	0	[VIIa]	$1.0075 \cdot 10^{-8}$
[TF = VIIa]	0	[Xa]	0
[IIa]	0	[X]	$6.8197 \cdot 10^{-11}$
[TF = VIIa = X]	0	[TF = VIIa = Xa]	0
[IX]	$6.9963 \cdot 10^{-8}$	[TF = VIIa = IX]	0
[VIII]	0	[VIIIa]	$1.7875 \cdot 10^{-12}$
[IXa]	0	[IXa = VIIIa]	0
[IXa = VIIIa = IX]	0	[VIIIa ₁ · L]	$6.9821 \cdot 10^{-10}$
[VIIIa ₂]	$6.9821 \cdot 10^{-10}$	[V]	$1.0000 \cdot 10^{-13}$
[Va]	$1.9999 \cdot 10^{-8}$	[Xa = Va]	0
[II]	0	[Xa = Va = II]	0
[mIIa]	0	[Xa = Va = II]	$2.5000 \cdot 10^{-9}$
[Xa = TFPI]	0	[TF = VIIa = Xa = TFPI]	0
[ATIII]	$1.8200 \cdot 10^{-6}$	[Xa = ATIII]	$1.5993 \cdot 10^{-7}$
[mIIa = ATIII]	$8.2640 \cdot 10^{-7}$	[IXa = ATIII]	$2.0037 \cdot 10^{-8}$
[IIa = ATIII]	$5.7360 \cdot 10^{-7}$	[TF = VIIa = ATIII]	$2.5000 \cdot 10^{-11}$

4.2 Varying Initial Conditions

Conditions that upset the balance in the proteins involved in coagulation may lead to various hemorrhagic or thrombotic diseases [1]. These conditions can be simulated with our model by changing the initial concentrations of certain protein species and looking at the change in thrombin production. This can give valuable information for the treatment hemostatic disorders.

Hemophilia A is a coagulation disorder that results from factor VIII deficiency and leads to longer

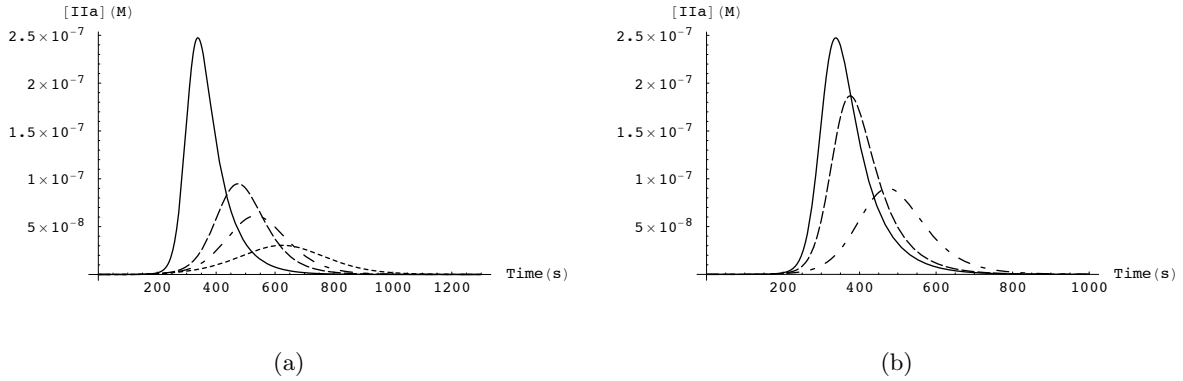


Fig. 4: Thrombin concentration as a function of time for (a) various VIII initial concentrations and (b) various IX initial concentrations. For graph (a), the normal VIII initial concentration is $0.7 \cdot 10^{-9}$ M (solid) and the hemophiliac VIII initial concentrations are $0.07 \cdot 10^{-9}$ M (---), $0.03 \cdot 10^{-9}$ M (- -), and $0.006 \cdot 10^{-9}$ M (- -). For graph (b), the normal IX initial concentration is $9 \cdot 10^{-8}$ M (solid) and the hemophiliac IX initial concentrations are $4.5 \cdot 10^{-8}$ M (---), and $1 \cdot 10^{-8}$ M (- -).

clotting time. Having less than 1 % of the normal amount of VIII in the blood stream can lead to spontaneous bleeding into joints and muscles, having 1-5 % of the normal amount of VIII in the blood stream can lead to occasional bleeding into joints and muscles and severe bleeding after minor injury, and having 5-25 % of the normal amount of VIII in the blood stream can lead to severe bleeding after major injury [9]. These 3 cases of hemophilia A are simulated with our mathematical model (Fig. 4a). It can be seen that decreasing the amount of VIII initially in the blood stream results in a lower maximum amount of thrombin produced and this maximum is reached at later times. Equilibrium is also reached at later times with lower initial VIII concentration.

Hemophilia B is a coagulation disorder that results from factor IX deficiency and leads to longer clotting time. Hemophilia B is simulated by decreasing the initial amount of IX in our mathematical model and looking at the thrombin concentration in the blood stream (Fig. 4b). It can be seen that decreasing the amount of IX initially in the blood stream results in a lower maximum amount of thrombin produced and this maximum is reached at later times. Equilibrium is also reached at later times with lower initial IX concentration.

It could be expected that factor VII would promote thrombin production because it is activated in the coagulation cascade to become VIIa. However, VII also takes part in the competition for TF with VIIa. It has been experimentally observed that factor VII inhibits thrombin production, proving that the competition for TF dominates VII activation [2]. The effect of the initial concentration of VII in the blood stream on thrombin production is examined with our model (Fig. 5a). It can be seen that as the initial concentration of VII increases the maximum amount of thrombin in the blood stream decreases and this maximum occurs at later times. Equilibrium is also reached later with increased VII concentration. This suggests that addition of factor VII in the blood stream would not be an effective treatment for hemophilia.

The effect of VIIa initial concentration on the thrombin concentration in the blood stream is examined (Fig. 5b). It is found that increasing VIIa initial concentration increases the maximum amount of thrombin in the blood stream and this maximum is found at earlier times. Equilibrium is also found at earlier times

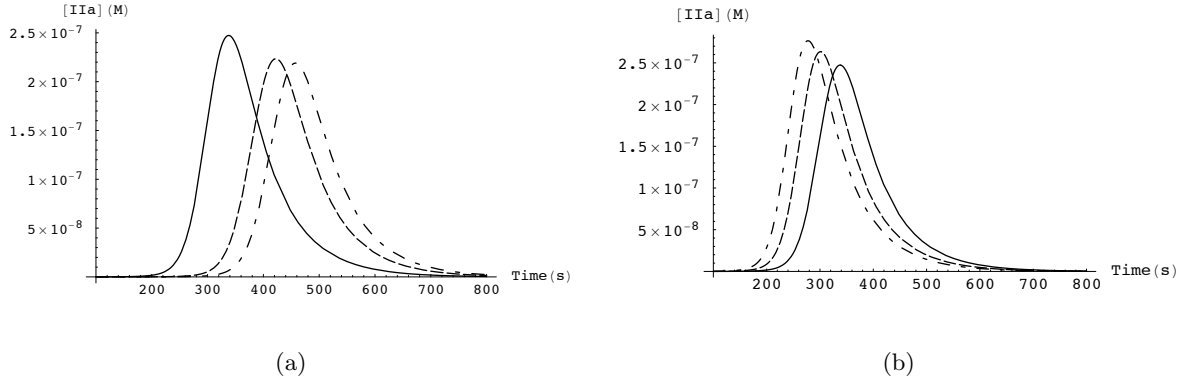


Fig. 5: Thrombin concentration as a function of time for (a) various VII initial concentrations and (b) various VIIa initial concentrations. For graph (a), the VII initial concentration are $1 \cdot 10^{-8}$ M (solid), $2.5 \cdot 10^{-8}$ M (---), and $3.5 \cdot 10^{-8}$ M (- -). For graph (b), the VIIa initial concentrations are $1 \cdot 10^{-10}$ M (solid), $1.5 \cdot 10^{-10}$ M (---), and $2 \cdot 10^{-8}$ M (- -).

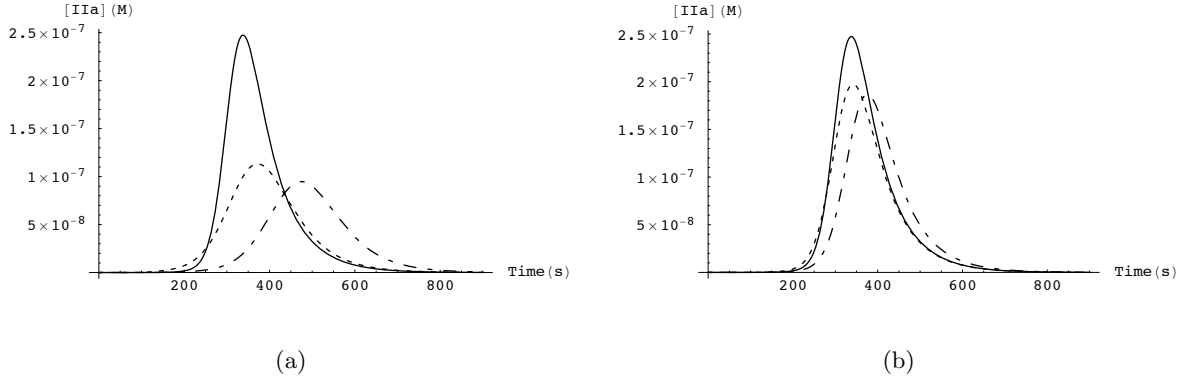


Fig. 6: Treatment with VIIa of (a) hemophilia A and (b) hemophilia B. For graph (a), we graph thrombin concentration versus time for a healthy person (solid), for a hemophiliac with $0.07 \cdot 10^{-9}$ M VIII concentration (---), and for a hemophiliac with $0.07 \cdot 10^{-9}$ M VIII concentration with VIIa levels raised to $2.5 \cdot 10^{-10}$ M (- -). For graph (b), we graph thrombin concentration versus time for a healthy person (solid), for a hemophiliac with $4.5 \cdot 10^{-8}$ M IX concentration (---), and for a hemophiliac with $4.5 \cdot 10^{-8}$ M VIII concentration with VIIa levels raised to $1.4 \cdot 10^{-10}$ M (- -).

with increased VIIa initial concentration. Patients suffering from hemophilia with factor VIII or IX inhibitors are given factor VIIa (Novoseven) as treatment [10]. Our mathematical model validates the treatment of hemophilia with VIIa.

The treatment of hemophilia A and B with factor VIIa is simulated (Fig. 6a and Fig. 6b). While it is possible to achieve the same lag phase of thrombin generation in hemophiliacs as for healthy people by the addition of VIIa, it is not possible to achieve both the same lag phase and the same maximum thrombin concentration. When the same lag phase is achieved, the maximum thrombin concentration remains lower in hemophiliacs treated with VIIa than in healthy people. This shows that VIIa therapy is less effective than the replacement of VIII or IX and should only be used in patients with VIII or IX inhibitors.

Antithrombin III deficiency is a condition that can lead to thrombosis [1]. This condition is simulated

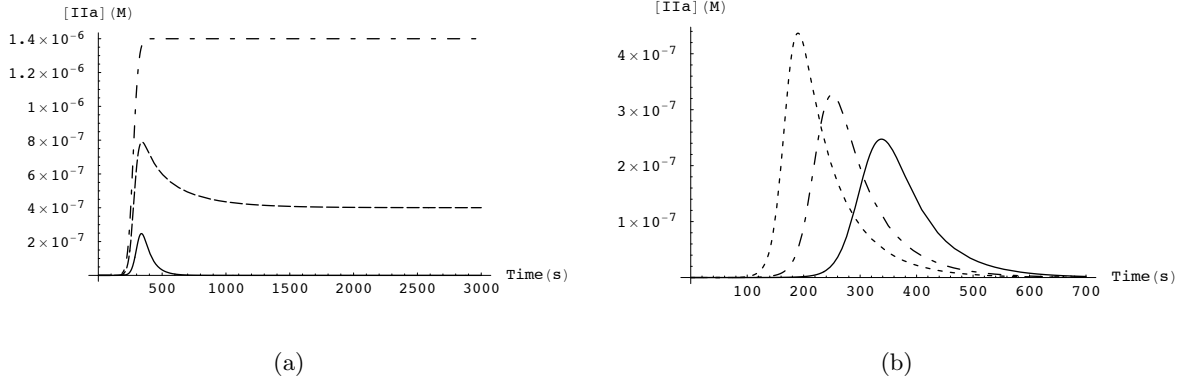


Fig. 7: Thrombin concentration as a function of time for (a) various antithrombin III initial concentrations and (b) various TFPI initial concentrations. For graph (a), the normal antithrombin III initial concentration is $3.4 \cdot 10^{-6}$ M (solid) and the deficient antithrombin III initial concentrations are $1 \cdot 10^{-6}$ M (---), and 0 M (- -). For graph (b), the normal TFPI initial concentration is $2.5 \cdot 10^{-9}$ M (solid) and the deficient TFPI initial concentrations are $1 \cdot 10^{-9}$ M (---), and 0 M (- -).

with our model by decreasing the initial concentration of antithrombin III and graphing the time dependent thrombin concentration (Fig. 7a). TFPI deficiency is also simulated by decreasing the initial TFPI concentration (Fig. 7b). Decreasing the initial antithrombin III concentration leads to a higher maximum thrombin concentration and a higher equilibrium thrombin concentration. Decreasing the initial TFPI concentration leads to a higher maximum thrombin concentration and this maximum is achieved at earlier times. Equilibrium is also achieved earlier with lower TFPI initial concentration.

4.3 Invariant Low-Dimensional Manifolds and Time-Scales

The existence of an attracting invariant one-dimensional manifold is suggested by several projections of the phase space for the coagulation cascade (Fig. 8a and Fig. 8b). Several trajectories follow the same curve as they approach equilibrium.

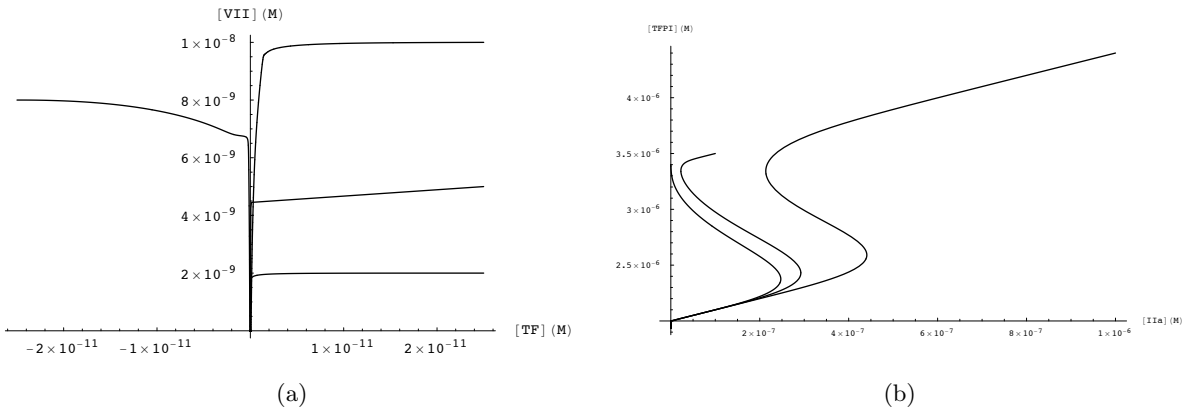


Fig. 8: (a) VII versus tissue factor concentration. (b) TFPI versus antithrombin III concentration.

The usefulness of using a one-dimensional manifold to simplify the system can be assessed by looking

at the separation of time-scales that characterize the system. One-dimensional manifolds are a useful simplification of the system if the longest time-scale is significantly larger than the other time-scales. This leads to all the time-scales, besides the longest one, having equilibrated for most of the reaction time. In order to assess the usefulness of using a one-dimensional manifold to simplify the blood coagulation model, the time-scales at equilibrium and also over the extent of the reaction time are determined. Near equilibrium, the time-scales are

$$\begin{aligned} \tau = \{ & 17736.8073, 11244.5905, 2375.5664, 2353.4060, 1125.2483, \\ & 322.5807, 166.2005, 165.8176, 77.3871, 77.3871, 4.2669, \\ & 0.2041, 0.1418, 0.1219, 0.1218, 0.050507, 0.006006 \} \text{ sec.} \end{aligned} \quad (65)$$

Only 17 time scales are given since the other 7 time scales are infinite. The infinite time-scales indicate that the linearized equations in the form of equation (5) are not an independent set and can be simplified to obtain 7 algebraic constraints. These 7 algebraic constraints indicate species conservation near equilibrium.

The time-scales from the start of the reaction to 40000 seconds are examined (Fig. 9). It can be seen that between 4000 and 40000 seconds, there is at least a factor of 4 difference between the longest and second longest time-scale, suggesting that there is a large domain where only the largest time-scale dominates. The second longest time-scale does not influence the system dynamics between 4000 and 40000 seconds because it does not rise above 4000 seconds in this domain. Therefore, it is possible that the trajectories of the system leading to the same equilibrium follow an invariant one-dimensional manifold in this domain. It can also be seen from equation (65) that near equilibrium the two longest time-scales are close to each other in size (less than a factor of 2 difference). This would indicate that the one-dimensional manifold is not a useful simplification of the system near equilibrium since two time-scales exert about an equal influence in this domain. However, while the time-scales still change at 40000 seconds, the concentrations are near equilibrium at this point and the one-dimensional manifold contains all the information needed to approximate the system after 4000 seconds.

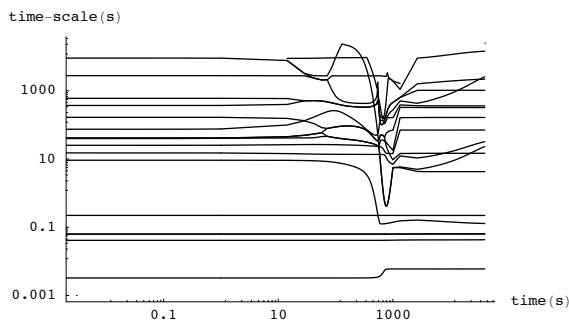


Fig. 9: Time-scales of the coagulation cascade as a function of time.

In order to verify that an attracting invariant one-dimensional manifold exists, the eigenvalues, λ_i , have to be examined in the time domain where the manifold is thought to influence the system dynamics. It is confirmed that all the eigenvalues are either negative or 0 after 1000 seconds, and hence an attracting invariant one-dimensional manifold exists. Negative eigenvalues indicate that moving away from the manifold

in any direction yields a fast relaxation back to the manifold.

The physical significance of the divergence is the rate at which density exits a given region of space. A negative divergence would indicate that density is accumulated in our system, which is consistent with the conclusion that as time increases, the trajectories collapse onto a one-dimensional path. The divergence of the system,

$$\text{div } \mathbf{f} = \nabla \cdot \mathbf{f}, \tag{66}$$

is calculated for the extent of the reaction time (Fig. 10). It can be seen from equation (4) that the trace of the Jacobian is the divergence of the system. The divergence can be found by adding the eigenvalues of the Jacobian since the trace of a square matrix is equal to the sum of its eigenvalues. It can be seen that the divergence is negative for the whole reaction time. This implies that the reaction space is contracting as the reaction proceeds, which is consistent with the trajectories collapsing onto a one-dimensional path.

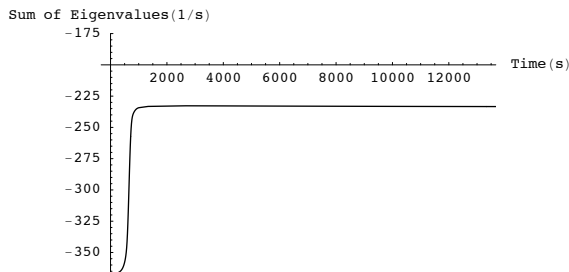


Fig. 10: The sum of the eigenvalues of the coagulation cascade as a function of time.

5 Conclusions and Future Work

The mathematical model proposed by Hockin et al. for coagulation is re-derived using the law of mass action. This mathematical model is used to obtain the time-dependent concentrations of the protein species involved in coagulation. Various hemostatic disorders are modeled and treatments simulated by changing the initial conditions of the system. Hemophilia A and B and AT-III and TFPI deficiency are at minimum successfully modeled qualitatively. The inhibitory effects on thrombin production of increasing VII initial concentration is shown and the treatment of hemorrhagic disorders with factor VIIa is validated. The existence of an attracting one-dimensional manifold that provides a useful approximation of the system after 4000 seconds is suggested by projections of the phase space and time-scale and eigenvalue analysis.

A useful extension of this work would be to integrate between the stable and unstable equilibria of the system to find one-dimensional manifolds. This would require the use of tools that could find all the roots of our system. Alternatively, the ILDM method could also be used to find the attracting invariant one-dimensional manifold of the system [8]. Other possible future study could involve the study of the effect of changing the initial conditions on the equilibrium of the system and the study of the sensitivity of the equilibrium to such changes.

References

- [1] Hockin M. F., Jones K. C., Everse S. J., and Mann K.G. (2002) *J. Biol. Chem.* **277**, 18322-18333
- [2] vant Veer, C., Golden, N. J., and Mann, K. G. (2000) *Blood* **95**, 1330-1335
- [3] Jones, K. C., and Mann, K. G. (1994) *J. Biol. Chem.* **269**, 23367-23373
- [4] van Dam-Mieras, M. C. E., and Muller, A. D. (1995) in *Blood Coagulation* (Zwaal, R. F. A., and Hemker, H. C., eds), pp. 1-13, Elsevier, Inc., New York
- [5] Lawson, J. H., Kalafatis, M., Stram, S., and Mann, K. G. (1994) *J. Biol. Chem.* **269**, 23357-23366
- [6] Powers, J. M., and Paolucci, S. (2005) *AIAA Journal* **43**, 1088-1099
- [7] Eggels, R. L. G. M., Louis, J. J. J., Kok J. B. W., De Goey, L.P.H. (1997) *Combust. Sci. and Tech.* **123**, 347-362
- [8] Maas, U., and Pope, S. B. (2005) *Combustion and Flame* **88**, 239-264
- [9] Black's Medical Dictionary (Marcovitch, H., eds) 41th Ed., pp. 331, Scarecrow Press, Inc., Lanham, Maryland

Appendix

